Special runs for diffractive measurements at the LHC

In this document, we describe briefly the different measurements that can be accomplished at the LHC using special runs. We will not mention the CT-PPS data taking that happens for the full LHC luminosity (anomalous coupling studies...). We assume two kinds of data taking:

- Very low luminosity for total cross section measurements
- Medium luminosity for $\beta^* \sim 90$ m

We propose the following list of runs to be taken at the LHC in order to perform the full set of measurements:

- High β^* runs in order to measure the elastic and total cross sections at 0.9, 2 and 14 TeV when available
- Medium β^* ($\sim$90 m) in order to perform QCD analysis of the pomeron structure and low mass SUSY studies
- standard data taking for CT-PPS/AFP for exploratory physics and for LHCb for the study of exclusive diffraction

In this short document, we will not mention further the high luminosity program since it will be given "for free" without the request of special runs at the LHC.

1 Total cross section measurement at 2 TeV and 14 TeV

The total cross section, the inelastic cross section and the elastic cross section have been measured by the TOTEM and ATLAS collaboration using Roman Pots in special high beta runs at 7, 8 and 13 TeV. Both experiments have published results at 7 TeV and 8 TeV and are analyzing the data that already has been taken at 13 TeV. From measurements of the differential elastic cross section at small t-values the total cross section, the inelastic cross section and the elastic cross section are derived. The inelastic cross section has also been measured by all the other LHC experiments with techniques not using Roman Pots but the far most precise measurement are coming from the Roman Pot data of TOTEM and ATLAS. In addition to the cross section measurements, TOTEM and ATLAS also measure the exponential slope of the differential elastic cross section, B. The different cross sections mentioned above and the slope parameter B are all global quantities characterizing the strong interaction and their evolution with $\sqrt{s}$ is always to be measured. The data so far indicates a continuation of an $ln^2 s$ behavior thus saturating the Froissart limit. Concerning the B parameter both TOTEM and ATLAS have observed a faster increase with $\sqrt{s}$ than was observed at lower energies. This has consequence for the phenomenological descriptions that are using Regge Field Theory to describe soft interactions. New data at low energies (typically 1- 2 TeV) and 14 TeV will allow to increase the lever arm for the energy evolution of all these quantities within one

experiment. Moreover a measurement at 2 TeV might be able to sort out the large discrepancy between the two data points of the total cross section measured at the Tevatron.

Both TOTEM and ATLAS can also measure elastic scattering at very small t-values (smaller than 10^{-3} GeV^2) Such small t-values allows a measurement of the ρ-parameter i.e. the real to imaginary part of the elastic scattering amplitude in the forward direction. The $\sqrt{s}$ evolution of the ρ-parameter has an interest in itself. In addition the ρ-parameter relates to the total cross section via dispersion relations. Dispersion relations are based upon model independent fundamental principles like analyticity and causality. Measuring the ρ-parameter at highest possible energy makes it possible to make predictions of the energy dependence of the total cross section beyond the energy at which it has been measured. On the other hand, a low energy measurement of the ρ-parameter at 1- 2 TeV could be used to validate the use of dispersion relations in the TeV range.

The energy of 2 TeV (or lower) would have a special interest related to the fact that measurements exist at 2 TeV from the Tevatron but in this case for anti-proton proton scattering. Proton-proton scattering and anti-proton scattering have not been measured at the same energy since ISR -times where a measurement of anti-proton proton scattering was performed at 52 GeV. Comparison of anti-proton scattering with proton scattering might give information on the up to now elusive C=-1 partner of the Pomeron i.e. the Odderon.

A measurement at lowe energies may be even more interesting. Of course, the total cross section has already been measured at 2.7 TeV. This is very close to the Tevatron energy and the main motivation to go to 2 TeV or even lower energies is ρ. The ρ measurement for $p\bar{p}$ at Tevatron suffers from a large error bar; hence it is not useful for direct comparison with a future pp measurement. Hence the TOTEM strategy is to go as close as possible towards the nearest existing $p\bar{p}$ measurement with reasonable precision, i.e. the UA4/2 point at 541 GeV. While going so low in energy at the LHC (half the usual injection energy) may not be possible (but is investigated), a 900 GeV measurement lies reasonably close and is possible. There the measurements of both σ_tot and ρ would have maximum impact.

2 Determination of the Pomeron structure

In this section, we discuss the measurements in CMS-TOTEM/ATLAS that can constrain the Pomeron structure. The existence of diffractive events where protons are intact in the final state is explained by the exchange of a colorless object called the Pomeron. In hard perturbative QCD, the Pomeron can be assumed of being made of quarks and gluons (at lowest order, it can be two gluons in order not to have any color exchange). The Pomeron structure in terms of quarks and gluons has been derived from QCD fits at HERA and at the Tevatron [1] and it is possible to probe this structure and the QCD evolution at the LHC in a completely new kinematical domain. All the following studies have been performed using the Forward Physics Monte Carlo (FPMC), a generator that has been designed to study forward physics, especially at the LHC [2]. It aims to provide a variety of diffractive processes in one common framework, *i.e.* single diffraction, double pomeron exchange, central exclusive production and two-photon exchange.

2.1 Dijet production in double Pomeron exchanges processes

Tagging both diffractive protons in CMS-TOTEM/ATLAS will allow the QCD evolution of the gluon and quark densities in the Pomeron to be tested and compared with the HERA measurements.

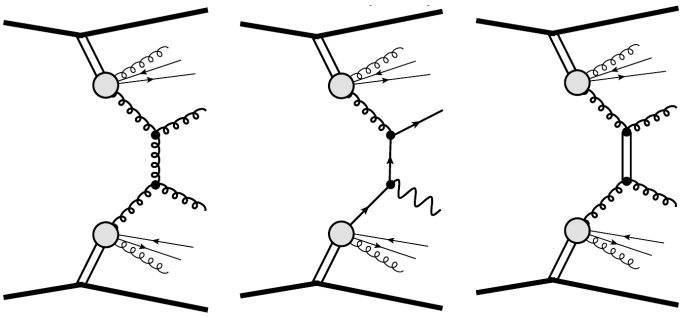

Figure 1: Inclusive diffractive diagrams. From left to right: jet production in inclusive double pomeron exchange, γ+jet production in DPE, dijet with a rapidity gap events

In addition, it is possible to assess its gluon and quark densities using the dijet and $\gamma + jet$ productions [3]. The different diagrams of the processes that can be studied at the LHC are shown in Fig. 1, namely double pomeron exchange (DPE) production of dijets (left), of γ+jet (middle), sensitive respectively to the gluon and quark contents of the Pomeron, and dijets with a rapidity gap events (right).

An observable sensitive to the gluon density in the Pomeron is displayed in Fig. 2. This is the so called dijet mass fraction [4], the ratio of the dijet mass to the total diffractive mass computed as $\sqrt{\xi_1 \xi_2 s}$ where $\xi_{1,2}$ are the proton fractional momentum carried by each Pomeron (as measured in the TOTEM proton detectors) and $\sqrt{s}$ the center-of-mass energy of 14 TeV. The central black line displays the cross section value for the gluon density in the Pomeron measured at HERA including an additional survival probability of 0.03. The yellow band shows the effect of the 20% uncertainty on the gluon density taking into account the normalization uncertainties. The dashed curves display how the dijet cross section at the LHC is sensitive to the gluon density distribution especially at high β. For this sake, we multiply the gluon density in the Pomeron from HERA by $(1-\beta)^\nu$ where ν varies between -1 and 1. When ν is equal to -1 (+1), the gluon density is enhanced (decreased) at high β.

We note that the curves corresponding to different values of ν are much more separated at high values of the dijet mass fraction, meaning that this observable is indeed sensitive to the gluon density at high β. This is due to the fact that the dijet mass fraction is equal to $\sqrt{\beta_1 \beta_2}$ where $\beta_{1,2}$ are the Pomeron momentum fraction carried by the parton inside the Pomeron which interacts. The measurement of the dijet cross section as a function of the dijet mass fraction is thus sensitive to the product of the gluon distribution taken at β_1 and β_2 [4].

2.2 Sensitivity to the Pomeron structure in quarks using γ+jet events

The aim of this study is twofold: is the Pomeron universal between HERA and the LHC and what is the quark content of the Pomeron? The QCD diffractive fits performed at HERA assumed that $u = d = s = \bar{u} = \bar{d} = \bar{s}$, since data were not sensitive to the difference between the different quark components in the Pomeron. The LHC data will allow us to determine which value of d/u is favored by data. Let us assume that $d/u = 0.25$ is favored. If this is the case, it will be needed to go back to the HERA QCD diffractive fits and check if the fit results at HERA can be modified to take into account this assumption. If the fits to HERA data lead to a large χ^2, it would indicate that

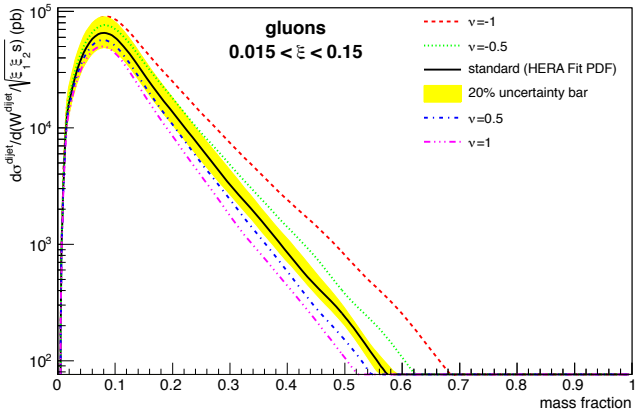

Figure 2: DPE di-jet differential cross section as a function of di-jet mass fraction distribution. The different curves correspond to different modifications of the Pomeron gluon density extracted from HERA data (see text).

the Pomeron is not the same object at HERA and the LHC. On the other hand, if the HERA fits work under this new assumption, the quark content in the Pomeron will be further constrained.

Fig. 3, displays the γ+jet to dijet cross section ratio as a function of the diffractive mass M computed from the proton ξ measured in the forward detectors $M = \sqrt{\xi_1 \xi_2 S}$ where ξ_1 and ξ_2 are the momentum fractions of the proton carried by each Pomeron and measured in the proton detectors [3]. It is displayed for different assumptions on the quark content of the Pomeron, d/u varying between 0.25 and 4 in steps of 0.25. We notice that the cross section ratio varies by a factor 2.5 for different values of u/d. The advantage of this variable is that most of systematic uncertainties due to the measurement of the diffractive mass cancel in the ratio since the mass distributions for γ+jet and dijet are similar. The typical resolution on mass is in addition very good, of the order of 2 to 3%. This measurement will be fundamental to constrain in the most precise way the Pomeron structure in terms of quark densities, and to test the Pomeron universality between the Tevatron and the LHC.

Let us notice that the measurement can be performed with about 50 pb^{-1} (about two weeks of data taking at a β^* $\sim$90 m).

In addition, it is possible to use the W asymmetry in single diffractive W production [5]. Typically, the muon asymmetry is directly sensitive to the quark content of the pomeron and varies by a factor 6 at low ξ between the assumptions $u/d = 2$ or $u/d = 1/2$ for the quark content in the pomeron.

Soft color interaction models (SCI) represent an additional model to describe diffraction. They describe [6] additional interactions between colored partons below the conventional cutoff for perturbative QCD. These are based on the assumption of factorization between the conventional perturbative event and the additional non-perturbative soft interactions. Soft exchanges imply that the changes in momenta due to the additional exchanges are very small, whereas the change in the event's color topology due to exchanges of color charge can lead to significant observables, e.g.

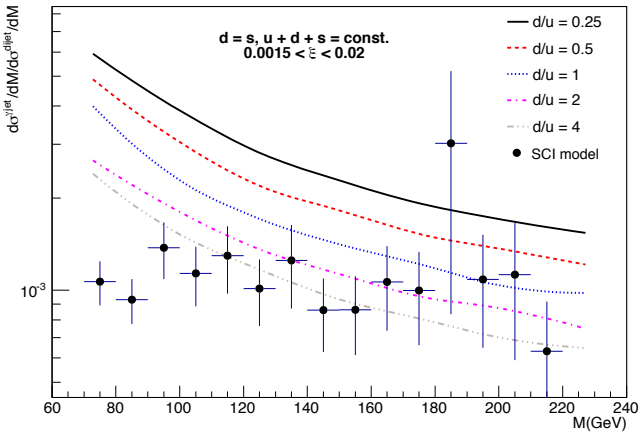

Figure 3: DPE $\gamma+$ jet to di-jet differential cross section ratio, in the acceptance of the proton detectors. as a function of diffractive mass, compared in addition to expectations from SCI models.

rapidity gaps and leading beam remnants. The probability to obtain a leading proton at the LHC in the context of SCI models depends on the color charge and the kinematic variables of the beam remnant before hadronization. The distribution of the γ+jet to the dijet cross section ratio as a function of the total diffractive mass distributions may allow to distinguish between the Pomeron and SCI models [3] since the latter leads to a more flat dependence on the total diffractive mass, as shown in Fig. 3.

3 Measurements of gap between jets in diffractive events

3.1 Principle of measurement

Fig. 4 shows the different evolutions in QCD in the $(Q^2, 1/x)$ plane where Q^2 and x are respectively the exchanged energy squared and the proton fractional momentum carried by the parton that interacts. The usual evolution equation that describes how the quark and gluon densities inside the proton evolve as a function of energy in terms of quark and gluon densities is the Dokshitzer Gribov Lipatov Altarelli Parisi [7] (DGLAP) one. The next-to-leading order or next-to-next-leading-order DGLAP evolution equation describes many cross section measurements at the LHC such as jets, WW, ZZ, $t\bar{t}$ productions. The other evolution equation called Balitsky Fadin Kuraev Lipatov [9] (BFKL) describes the evolution in x. The aim of our proposal is to study this dynamics at low x, specifically:

- Study the predictions of BFKL resummation in dedicated measurements such as the jet gap jet cross section in diffractive events
- Study the new regime of QCD where the density of gluons becomes very large in pA collisions described in the next section.

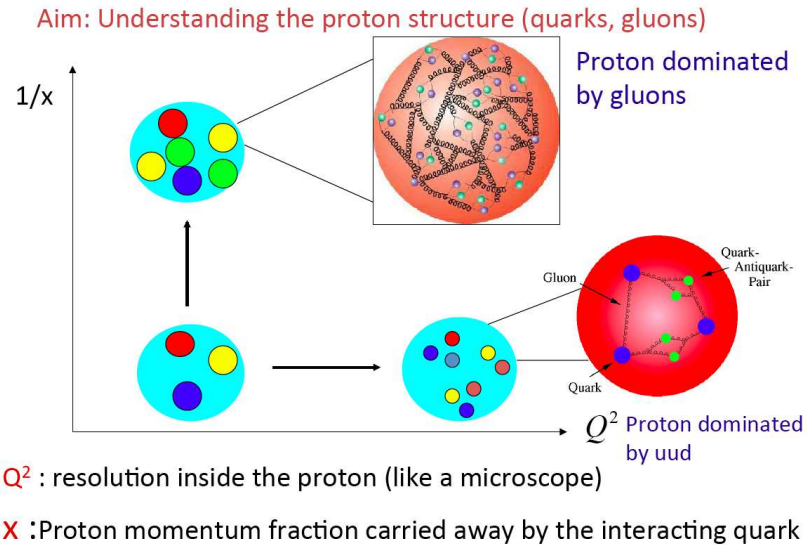

Figure 4: Evolution equations in QCD. We distinguish between the evolution in energy or in Q^2 of the parton densities in the proton called the Dokshitzter Gribov Lipatov Altarelli Parisi (DGLAP) evolution equation and the Balitski Fadin Kuraev Lipatov evolution in x.

3.2 Measuring jet gap jet events in diffraction at the LHC

While many measurements sensitive to BFKL resummation effects have already been performed in the past at the Tevatron and the LHC [10], they have never led to a clear signal of BFKL resummation since they are sensitive to higher order QCD effects that are difficult to disentangle.

In this proposal, we aim at measuring events with a gap in rapidity devoid of any energy deposition between jets in diffractive events at the LHC. The rapidity gap is the signature of the exchange of a colorless object called a Pomeron between the two jets. The intact protons in the final state are measured in the CMS-TOTEM/ATLAS Forward Proton Detectors and the two jets inside the CMS/ATLAS central detectors. In addition, we assume a rapidity gap $\Delta\eta$ between the two jets. The advantage of this measurement is that it is very clean and would lead to a clear signal of BFKL resummation effects as we will see in the next subsection.

3.3 BFKL formalism

The production cross section of two jets with a gap in rapidity between them reads [11, 12]

$$\frac{d\sigma^{pp\to XJJY}}{dx_1 dx_2 dE_T^2} = \mathcal{S} f_{eff}(x_1, E_T^2) f_{eff}(x_2, E_T^2) \frac{d\sigma^{gg\to gg}}{dE_T^2}, \tag{1}$$

where E_T is the transverse energy of the two jets, x_1 and x_2 their longitudinal fraction of momentum with respect to the incident hadrons, S the survival probability for the gap, and f the effective parton density functions [12]. The rapidity gap between the two jets is $\Delta\eta = \ln(x_1 x_2 s/p_T^2)$.

The cross section is given by

$$\frac{d\sigma^{gg\to gg}}{dE_T^2} = \frac{1}{16\pi}\left|A(\Delta\eta, E_T^2)\right|^2 \tag{2}$$

in terms of the $gg \to gg$ scattering amplitude $A(\Delta\eta, E_T^2)$.

In the following, we consider the high energy limit in which the rapidity gap $\Delta\eta$ is assumed to be very large. The BFKL framework allows to compute the $gg \to gg$ amplitude in this regime, and the result is known up to NLL accuracy (see Formula (2) of Ref. [11]).

In this study, we performed a parametrized distribution of $d\sigma^{gg\to gg}/dE_T^2$ so that it can be efficiently implemented in the Herwig Monte Carlo [14]. The implementation of the BFKL cross section in a Monte Carlo is absolutely necessary to make a direct comparison with data. For example, since the measurements are sensitive to the jet size, the gap size is different from the rapidity interval between the jets which is not the case by definition in the analytic calculation.

3.4 Experimental observable and discussion

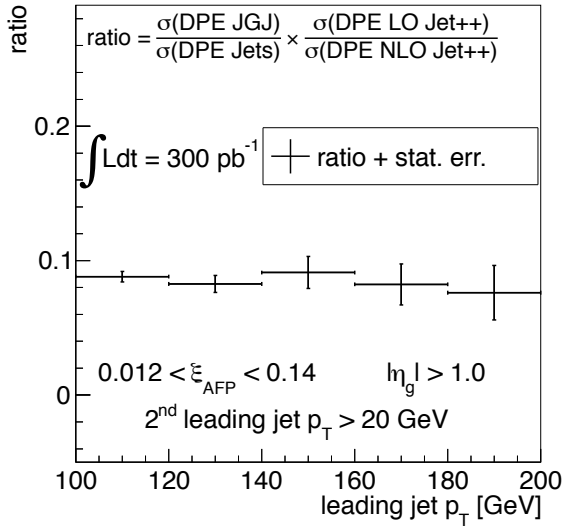

Figure 5: Simulation of the ratio of the jet-gap-jet to the inclusive jet cross sections at the LHC as a function of jet p_T in double pomeron exchange events where the protons are detected in TOTEM in pp collisions at 13 TeV at the LHC. The gap devoid of energy in the CMS/ATLAS detectors is between (-1) and (1) in rapidity ($|\eta_g| > 1$) and the protons are assumed to be detected in TOTEM for standard running (the fraction of the proton momentum carried by the Pomeron is between $0.012 < \xi < 0.14$). The systematics originate mainly for jet energy scale uncertainties assumed to be of the order of 2%. A moderate luminosity of 300 pb^{-1} is assumed.

The idea is to tag the intact protons inside the CMS-TOTEM/ATLAS forward proton detectors [8] (Roman Pots) located at about 220 m from the CMS/ATLAS interaction point on both sides. The advantage of such processes is that they provide clean experimental signatures since they are not "contaminated" by proton remnants and it is possible to go to larger jet separation

than the usual jet-gap-jet events. The ratio between jet-gap-jet to inclusive jet events is shown in Fig. 5. For this simulation, both protons were required to be reconstructed in the Roman Pots in standard high luminosity running at the LHC (called low β^* running where β^* is related to the beam lattice properties). The ratio shows a weak dependence in jet p_T (and also on the difference in rapidity between the two jets). It is worth noting that the ratio is about 20-30% showing that the jet-gap-jet events are much more present in the diffractive sample than in the inclusive one which would be more of the order of a few per mil. The DGLAP resummation predictions for such events leads to a very small cross section and the observation of such events would be a clean signal of BFKL resummation for the first time at a collider.

4 Exclusive processes in diffraction

4.1 Glueballs and vector mesons

The advantage of the exclusive diffractive and photon exchange processes is that all particles can be measured in the final state. Both protons can be measured in CMS-TOTEM/CT-PPS/ATLAS and the produced particles (jets, vector mesons, Z boson, etc) in CMS/ATLAS, and there is no energy losses such as in the pomeron remnants. It is thus possible to reconstruct the properties of the object produced exclusively (via photon and gluon exchanges) from the tagged proton since the system is kinematically constrained. It is worth mentioning that it is also possible to constrain the background by requesting the matching between the information of the two protons and the produced object, and thus, central exclusive production is a potential channel for beyond standard model searches at high masses.

For instance, the CMS-TOTEM/ATLAS experiments performed extensive studies of possible measurements of exclusive states at high β^*. It is worth mentioning that the search for glueball states and the probe of the low x gluon density down to $x \sim 10^{-4}$ will be possible [8]. It is possible to discover or exclude glueballs at low masses since the 1-10 GeV region in masses can be probed diffractively ($\xi \sim 10^{-4} - 10^{-3}$), ensuring pure gluonic exchanges. It is then possible to check the $f_0(1500)$ or $f_0(1710)$ glueball candidates (lattice calculations predict a 0^{++} glueball at 1.7 GeV with a $\sim$100 MeV uncertainty, favoring the $f_0(1710)$ candidate). The simulation of a possible signal of $f_0(1710) \to \rho^0\rho^0$ and of the non resonant $\rho^0\rho^0$ background including the CMS tracker performance leading to a 20-30 MeV resolution was performed and a luminosity of ~ 0.06 pb^{-1} is needed for a 7 σ signal. About 0.6 pb^{-1} is needed for decay characterization In addition, it is possible to perform a spin analysis of $f_0(1710) \to \rho^0\rho^0 \to 4\pi$ to determine if $J = 0$ or 2: as an example, a measurement of the polar angle of the $\pi^+\pi^-$ pair for the ρ candidate needs about 5 pb^{-1} of data. It is worth noticing that many data looking for glueballs have been taken and are being analyzed.

4.2 Search for missing mass and momentum candidates

CD provides simultaneous and precise measurement of the initial and final state kinematics, which can be used to search for events with missing mass or missing momentum signatures. This opens up ways for new physics searches that might have escaped the searches of the general purpose detectors, CMS and ATLAS. Only CD events with a $M_{PF+P_{miss}} \leq M_X$ are examined to avoid contamination from pileup events. The rapidity gaps, $\Delta\eta = -\ln \xi$, predicted by the proton ξ measurements are verified using the T2 detector with a rapidity coverage of $5.3 < |\eta| < 6.5$. To

probe O(pb) cross-sections, a statistics corresponding to an integrated $\beta^* = 90$ m luminosity of $\sim$ 50 pb^{-1} is needed.

The search signature is high missing momentum pointing towards a region with good CMS-TOTEM instrumentation ($|\eta| < 6.5$) and not observing charged particles or energy deposits in η regions close to where the missing momentum points, see Figure 6 (right). This happens if a particle is created in the CD reaction and escapes the detectors undetected. Events are rejected if rapidity gaps more forward than T2 would be allowed by the proton ξ measurements. For $\sqrt{s} = 13$ TeV, the search is confined to the 200-700 GeV/c^2 mass range, where the upper limit is due to the maximal central mass allowed by the T2 acceptance and the lowe limit due to ξ resolution. Events with missing momentum up to 400 GeV/c were found in the Run I data set with background events expected from particles escaping detection in the forward region, due to "acceptance gaps" between detectors as well as from $p + p \to N^* \oplus X \oplus p$ or $p \oplus X \oplus N^*$ reactions. In the latter case, one of the observed protons comes from a decay of a nucleon resonance, N^*, and the other N^* decays products escape detection. With increased statistics, it is expected that these backgrounds will be modeled sufficiently well.

An example process is squark $\tilde{q}\tilde{\bar{q}}$ pair production for one generation with $\tilde{q} \to q + \tilde{\chi}_1^0$ decay for $\tilde{q}$ masses of up to 200-220 GeV, where a central diffractive cross-section of 1-10 pb can be expected [15]. An integrated luminosity of $\sim$50 pb^{-1} could yield $\sim$10-100 events according to simulation studies with the missing energy being due to the two neutralinos ($\tilde{\chi}_1^0$). Such a search could allow to cross-check the current exclusion limits on the $m_{\tilde{q}} - m_{\tilde{\chi}_1^0}$ range without tight cuts on the centrally visible system, and especially explore the $m_{\tilde{q}} - m_{\tilde{\chi}_1^0} \leq$ 30-40 GeV/c^2 range in detail. The hypothesis of close $\tilde{q}$ and $\tilde{\chi}_1^0$ masses is particularly relevant for the supersymmetric top quark $\tilde{t}$ given the cosmological implications [16].

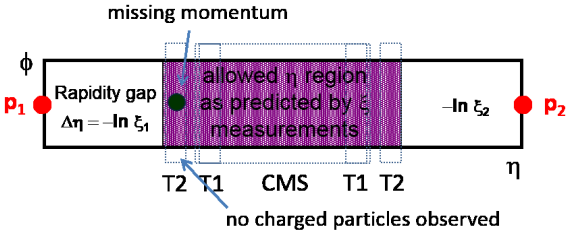

Figure 6: Schematical drawing of the the event topology used in the search for high missing momentum candidates.

References

[1] H1 Coll., Eur.Phys.J.C**48** (2006) 749; Eur.Phys.J.C**48** (2006) 715; C. Royon, L. Schoeffel, S. Sapeta, R. Peschanski, E. Sauvan, Nucl.Phys. B**781** (2007) 1.

[2] M. Boonekamp, A. Dechambre, V. Juranek, O. Kepka, M. Rangel, C. Royon, R. Staszewski, e-Print: arXiv:1102.2531; M. Boonekamp, V. Juranek, O. Kepka, C. Royon "Forward Physics Monte Carlo", "Proceedings of the workshop: HERA and the LHC workshop series on the implications of HERA for LHC physics," arXiv:0903.3861 [hep-ph].

[3] C. Marquet, C. Royon, M. Saimpert, D. Werder, Phys.Rev. D **88** (2013) 7, 074029.

[4] O. Kepka, C. Royon, Phys.Rev. D**76** (2007) 034012; CDF Coll., Phys. Rev. D **77**, (2008) 052004.

[5] A. Chuinard, C. Royon, R. Staszewski, JHEP 1604 (2016) 092.

[6] A. Edin, G. Ingelman and J. Rathsman, Phys. Lett. B **366**, 371 (1996); Z.Phys. C**75**, 57 (1997); J. Rathsman, Phys. Lett. B **452** (1999) 364.

[7] G.Altarelli and G.Parisi, *Nucl. Phys.* **B126** 18C (1977) 298; V.N.Gribov and L.N.Lipatov, *Sov. Journ. Nucl. Phys.* (1972) 438 and 675; Yu.L.Dokshitzer, *Sov. Phys. JETP.* **46** (1977) 641.

[8] TOTEM Coll., CERN-LHCC-2014-020; CMS and TOTEM Coll., CERN-LHCC-2014-021.

[9] V. S. Fadin, E. A. Kuraev, L. N. Lipatov, Phys. Lett. B**60** (1975) 50; I. I. Balitsky, L. N. Lipatov, Sov.J.Nucl.Phys. **28** (1978) 822.

[10] A. H. Mueller, H. Navelet, Nucl.Phys. B**282** (1987) 727.

[11] C. Marquet, C. Royon, M. Trzebinski, R. Zlebcik, Phys.Rev. D**87** (2013) no.3, 034010;

[12] O. Kepka, C. Marquet, C. Royon, Phys.Rev. D**83** (2011) 034036.

[13] T. Sjostrand, S. Mrenna and P. Z. Skands, Comput. Phys. Commun. **178** (2008) 852.

[14] G. Corcella et al., JHEP **0101** (2001) 010.

[15] TOTEM Coll., CERN-LHCC-2014-020; TOTEM-TDR-002, addendum: CERN-LHCC-2014-024; TOTEM-TDR-002-ADD-1.

[16] K. Huitu, L. Leinonen, J. Laamanen, Phys. Rev. D**84** (2011) 075021.